Discover Applied Sciences

Research

Entropy generation on MHD motion of hybrid nanofluid with porous medium in presence of thermo-radiation and ohmic viscous dissipation

Revathi Devi Murugan[1] · Narsu Sivakumar[1] · Nainaru Tarakaramu[2,3] · Hijaz Ahmad[4,5] · Sameh Askar[6]

Received: 26 November 2023 / Accepted: 27 March 2024
Published online: 06 April 2024

Abstract
Hybrid nanotechnology has significantly contributed to enhancing energy efficiency and reducing heat loss. This study addresses entropy analysis in the motion of hybrid nanofluids incorporating magnetohydrodynamic effects, thermal radiation, and ohmic viscous dissipation phenomena. The implementation of magnetohydrodynamic, thermal radiation, and dissipation effects allows for a second law of thermodynamics analysis. The hybrid nanoparticles considered are Graphene Oxide (GO) and Molybdenum Disulphide (MoS_2), with water serving as the base liquid. Entropy generation analysis, a thermodynamic approach, quantifies irreversibility and inefficiencies within the system, aiding in understanding losses and identifying areas for improvement. Additionally, a comparative study is conducted. The BVP4C algorithm, implemented using MATLAB, is employed to address this study and obtain solutions. The key findings indicate that heat transfer rates are higher for blade-shaped nanoparticles, and entropy is minimized by controlling parameters such as the radiation parameter, Brinkman parameter, and temperature difference.

Article Highlights

- This study aims to investigate the heat transfer rate, entropy rate, and Bejan number of various shapes of nanoparticles.
- The heat transfer rate of a hybrid nanoparticle is found to be higher than that of mono-particles.
- Controlling the radiation parameter and Brinkman number can minimize irreversibility caused by heat transfer and entropy generation.

Keywords Magnetohydrodynamic · Hybrid nanofluid · Entropy generation · Ohmic viscous dissipation · Thermal radiation · Porous

✉ Narsu Sivakumar, narsusic@srmist.edu.in | [1]Department of Mathematics, College of Engineering and Technology, SRM Institute of Science and Technology, Kattankulathur, Tamil Nadu 603 203, India. [2]Department of Mathematics, School of Liberal Arts and Sciences, Mohan Babu University, Sree Sainath Nagar, Tirupati, A.P 517102, India. [3]Department of Mathematics, School of Liberal Arts and Sciences, Sree Vidyanikethan Engineering College, Sree Sainath Nagar, Tirupati, A.P 517102, India. [4]Department of Mathematics, Faculty of Arts and Sciences, Near East University, Mersin 10, TRNC, Turkey. [5]Section of Mathematics, International Telematic University Uninettuno, Corso Vittorio Emanuele II, 39, 00186 Rome, Italy. [6]Department of Statistics and Operations Research, College of Science, King Saud University, P.O. Box 2455, 11451 Riyadh, Saudi Arabia.

Abbreviations

MHD	Magneto-hydro dynamics
MoS_2	Molybdenum disulphide
GO	Graphene oxide
HNF	Hybrid nano-fluid
NF	Nano-fluid
F	Fluid

List of symbols

c_p	Specific heat in constant temperature
σ^*	Stefan Boltzmann constant
k^*	Coefficient for absorption
B_0	Field of magnetism
M	Magnetic parameter
f	Stream function in dimensionless form
Rd	Radiation parameter
Pr	Prandtl number
Kp	Darcy parameter
Ec	Eckert number
Be	Bejan number
Ng	Entropy generation
Br	Brinkman number
Cf	Skin friction coefficient
Re_x	Local Reynolds number
Nu_x	Local Nusselt number
Q_0	Heat absorption or generation parameter
Q	Heat source/sink parameter
ε	Porosity term
u	Velocity field of x-direction (m s^{-1})
v	Velocity field of y-direction (m s^{-1})
q_r	Heat flux (J m^{-2} s^{-1})
T	Temperature at any point (K)
T_∞	Temperature for free stream (K)
T_w	Temperature at the wall (K)
ψ	Stream function (m^2 s^{-1})
η	Normal to the surface (dimensionless distance)
A	Constant to the surface temperature
g	Acceleration based on gravity
β_T	Coefficient of thermal expansion
m	Shape of the nanoparticle
K_{hnf}	Thermal conductivity for hybrid nano-fluid (W m^{-1} k^{-1})
K_{nf}	Thermal conductivity for nano-fluid (W m^{-1} k^{-1})
υ_{hnf}	Kinematic viscosity for hybrid nano-fluid (m^2 s^{-1})
υ_{nf}	Kinematic viscosity for nano-fluid (m^2 s^{-1})
ρ_{hnf}	Density for hybrid nano-fluid (kg m^{-3})
ρ_{nf}	Density for nano-fluid (kg m^{-3})
σ_{hnf}	Electric conductivity for hybrid nano-fluid (Ω m^{-1})
σ_{nf}	Electric conductivity for nano-fluid (Ω m^{-1})

1 Introduction

Thrust of emerging technology in the world paws a way for developing new technology. One such concept gaining traction in the scientific community is nanotechnology, often referred to as engineered fluids within the realm of fluid dynamics and heat transfer. The thermal conductivity of water and ethylene glycol (conventional fluid) have low values compared with thermal conductivity of nanoparticle. To attain this property, researchers have explored the concept of nanofluids—mixtures of base fluids and nanoparticles—which offer enhanced thermal conductivity. Adding nanoparticles to the base fluid improves its thermal properties. Choosing the right type of nanoparticles can significantly influence the thermal conductivity, viscosity, and other properties of the nanofluid. Foremost person who gave a different opinion to the scientific community and industrial area to enhance their development through nanoparticles was introduce Choi [1]. Hybrid nanofluids (HNFs), which combine traditional base fluids with nanoparticles, have emerged as a promising pathway for improving heat transfer rates over conventional single-component nanofluids. Researchers and engineers have delved into experimental studies to optimize HNF properties for specific applications, ranging from heat exchangers to electronics cooling systems and solar collectors.

Wong and Leon [2] provided insights into various applications of nanofluids, covering both current and future technologies. Subsequent studies by Yu and Xie [3] focused on nanofluid preparation, stability, and applications, while Shoaib et al. [4] investigated 3D radiative HNF motion via a rotational disk. Ratha et al. [5] explored the 2D unsteady motion of incompressible Casson nanofluids over a shrinking horizontal sheet.

The term 'hybrid material' refers to substances that blend the chemical and physical properties of multiple materials, offering unique qualities absent in their individual components. Two-step and single-step methods are employed to synthesize nanoparticles into HNFs. Various factors such as nanoparticle dispersion, purity levels, and synthesis methods can impact HNF efficiency. Mustafa [6] conducted an investigation using linear stability theory to analyze nanoparticles in a single-phase model.

Understanding the behavior of viscous fluids across different conditions requires a basic understanding of viscous dissipation principles, which are fundamental to fluid dynamics. It is the mechanism by which a fluid transfers mechanical energy into heat while flowing because of its natural viscosity. This phenomenon occurs due to internal friction between adjacent fluid layers, leading to a gradual loss of kinetic energy and a corresponding increase in temperature. Viscous dissipation is a crucial aspect of liquid motion analysis. Which influences various engineering and scientific applications (like, the cooling of electronic components, etc.). Ohmic viscous dissipation is an interesting mechanism that converts electrical energy in conductive fluids into heat due to electrical resistance. The effects of viscous dissipation on heat transfer in a cold liquid with a coupled stress mechanism were examined by Masthanaiah et al. [7]. Mahesh et al. [8] presented the impact of MHD coupled stress HNF through a porous surface with dissipation effect. Moreover, Sharma et al. [9] investigated the NF motion via rotating disk in moving up/down wards with viscous dissipation phenomena. Additionally, Rashad et al. [10] analyzed the variations of heat transfer by using Williamson HNF over a curved porous medium.

Internal heat generation and absorption is indeed crucial for analyzing, designing, and predicting temperature distributions in various systems, from power plants to refrigeration units. Internal heat generation refers to heat production within a system due to internal processes, while internal heat absorption involves heat transfer from the surroundings or within the system itself. This phenomenon is often encountered in systems such as power plants, electronic devices, chemical reactors, and even living organisms. Yaseen et al. [11] investigated the effect of shape on the flow of radiative hybrid nanofluids over a permeable sheet, observing an increase in heat transfer.

Absolutely, thermal radiation is a fundamental aspect of engineering, particularly in fields like HVAC (Heating, Ventilation, and Air Conditioning), materials science, and thermal engineering. Understanding how materials emit, absorb, and transmit thermal radiation is crucial for designing efficient heating and cooling systems, as well as for selecting appropriate materials for various applications. The homogeneous and heterogeneous chemical reactions on Bioconvection HNF with radiation effect was developed by Puneeth et al. [12]. subsequently, the heat transfer rate has been determined by Nayak et al. [13] by examining thermal radiation and heat dissipation effect on nanofluid motion.

Indeed, Magnetohydrodynamics (MHD) is a fascinating interdisciplinary field that merges principles of fluid dynamics and electromagnetism. It's concerned with the behavior of electrically conducting fluids, such as plasmas, liquid metals, and electrolytes, in the presence of magnetic fields. Mustafa et al. [14] examine the mixed convective flow of magnetonanofluid bounded by a vertical stretchable surface. Krishna et al. [15] explore unsteady magnetohydrodynamic (MHD) motion of a non-Newtonian Casson HNF over a vertically moving porous surface under slip velocity in a rotating frame.

The concept of a porous medium is fundamental across various fields due to its widespread occurrence and diverse applications. Here's how porous media impact different domains: Geosciences and Hydrology, Engineering and Civil Infrastructure, Chemical Engineering and Catalysis, Biomedical Applications, Environmental Science, Material Science and Manufacturing. Nandi et al. [16] investigate the flow of magneto-convective and chemically reactive Casson nanofluid along an inclined permeable stretching with saturated medium. The HNF magnetized between two coaxially rotated porous disks was investigated by Qureshi et al. [17]. Abad et al. [18] analyze the heat and mass transfer in HNF motion on a cylindrical bluff-body with effect of chemical reactions.

Entropy generation is a crucial topic in thermodynamics and engineering to understand the efficiency and irreversibility of energy and heat transmission systems. It plays an essential role in understanding energy transmission phenomena and directionalities of the physical process. The entropy can take on any value of negative, positive, or zero-but this one is always either zero or positive. The generation of entropy is possible but its destruction is impossible. According to 2nd law of thermodynamics, the rate of local entropy generation per unit volume can be estimated as $S'''_{gen} = \frac{k}{T_0^2}(\nabla T)^2 + \frac{\mu}{T_0}\phi + \frac{q'''}{T_0}$. The entropy generation mechanism finds application in various sectors such as air conditioners, heat pumps, and freezers. Recently, Bejan [19, 20] explained the entropy generation caused by heat transfer in convective mode across a stretching sheet. Baag et al. [21] investigated the production of entropy generation with convective heat and mass transfer effects. Some of the researchers [28, 29] published the HNF with nanoparticles GO and MoS_2 with different geometry, like cylinders and disks and also with different base fluids with different boundary conditions.

The present study aims to investigate the behaviour of hybrid nanofluids over a stretching sheet incorporating thermal radiation, heat source/sink, MHD, ohmic heating and viscous dissipation effects. By numerically solving using the BVP4C MATLAB solver, we aim to build upon the work of Pal et al. [17] and explore irreversibility mechanisms. This study holds implications for various fields, including medicine, where nanocomposites can serve as coolants in electronic devices and aid in cancer treatment through hyperthermia therapy. By optimizing energy efficiency and minimizing entropy generation, nanocomposites can contribute to more effective cancer treatments.

2 Mathematical model of the problem

We consider the steady, incompressible, two-dimensional magnetohydrodynamic (MHD) hybrid nanofluid (HNF) with two different types of nanoparticles namely Graphene-Oxide and Molybdenum-Disulphide over a stretching surface. The effects of heat source/sink, thermal radiation and Ohmic-viscous dissipation are taken into account. Additionally, T_w and T_∞ represents the wall temperature and ambient temperature, respectively. An external magnetic field B_o is applied in the normal direction to the liquid flow surface. The plane's surface is considered in the x-direction and normal plane is taken in y-direction as shown in Fig. 1. The governing non-linear partial differential equation for boundary layer with the Darcian flow of HNF through a porous medium as follows (ref. [22, 27]).

$$\frac{\partial u}{\partial x} + \frac{\partial v}{\partial y} = 0 \tag{1}$$

$$\frac{1}{\varepsilon^2}\left(u\frac{\partial u}{\partial x} + v\frac{\partial u}{\partial y}\right) = \frac{1}{\varepsilon}\frac{\mu_{hnf}}{\rho_{hnf}}\frac{\partial^2 u}{\partial y^2} - \frac{\sigma_{hnf}}{\rho_{hnf}}B_0^2 u - \frac{\mu_{hnf}}{\rho_{hnf}k_p}u \tag{2}$$

$$\left(u\frac{\partial T}{\partial x} + v\frac{\partial T}{\partial y}\right) = \frac{K_{hnf}}{(\rho c_p)_{hnf}}\frac{\partial^2 T}{\partial y^2} + \frac{\sigma_{hnf}}{(\rho c_p)_{hnf}}B_0^2 u^2 + \frac{\mu_{hnf}}{(\rho c_p)_{hnf}}\left(\frac{\partial u}{\partial y}\right)^2 - \frac{1}{(\rho c_p)_{hnf}}\frac{\partial q_r}{\partial y} + \frac{Q_0}{(\rho c_p)_{hnf}}(T - T_\infty) \tag{3}$$

Equation 3 represents the heat transported by a hybrid nanofluid through convection and conduction, wherein the magnetic field induces joule heating, viscous dissipation terms, heat generation and absorption, and radiation terms.

The boundary conditions in dimensional form are provided below [22, 27]:

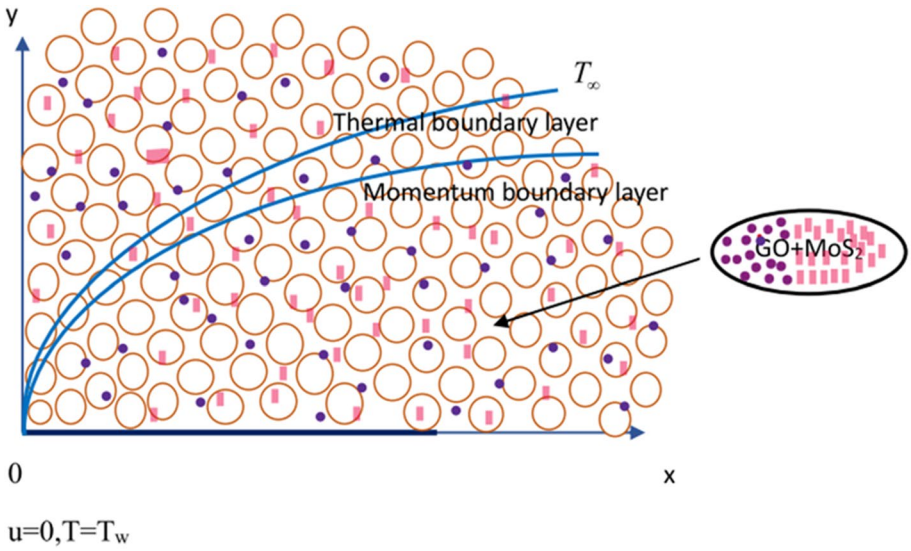

Fig. 1 Physical diagram of the problem

$$\begin{aligned} &u = 0, v = v_w, T = T_w \ at \ y = 0 \\ &u \to 0, T \to T_\infty \ as \ y \to \infty \end{aligned} \tag{4}$$

Here, the u value is set to zero, which represents the velocity of fluid particle vanishing at the solid boundary and it gradually increasing away for the surfaces to attain free stream velocity. Similarly, the fluid particles near to surface are at rest, heat is conducted from a solid surface into the fluid particle, causing a temperature gradient for them to reach the wall temperature.

Here, Radiative heat flux $q_r\left(=-\frac{4\sigma^*}{3k^*}\frac{\partial T^4}{\partial y}\right)$ is defined using Rosseland approximation.

The T^4 is expanded in terms of T_∞, by using the Taylor series is,

$$T^4 \approx T_\infty^4 - 4T_\infty^3\left(T - T_\infty\right) + 6T_\infty^2\left(T - T_\infty\right)^2 + \ldots \tag{5}$$

Here we omit the higher order of temperature difference,

$$T^4 \approx 4TT_\infty^3 - 3T_\infty^4,$$

Transformations for the proposed model is referred from Pal et al. [22] and its listed below,

$$\left.\begin{aligned} &u = \left(g\beta_T A\right)^{\frac{1}{2}} xf', v = -\left(g\beta_T A\upsilon_f^2\right)^{\frac{1}{4}} f, \eta = \left(\frac{g\beta_T A}{\upsilon_f^2}\right)^{\frac{1}{4}} y \\ &f = \frac{\psi}{\left(g\beta_T A\upsilon_f^2\right)^{\frac{1}{4}} x}, \theta = \frac{\left(T - T_\infty\right)}{\left(T_w - T_\infty\right)} \end{aligned}\right\} \tag{6}$$

Using the above transformation (5), Eq. (2) and (3) are changed as follows, and Eq. (1) is satisfied trivially,

$$\frac{1}{\varepsilon}\frac{\mu_{hnf}}{\mu_f}f''' + \frac{1}{\varepsilon^2}\frac{\rho_{hnf}}{\rho_f}\left(ff'' - f'^2\right) - \left(\frac{\sigma_{hnf}}{\sigma_f}M + \frac{\mu_{hnf}}{\mu_f}Kp\right)f' = 0 \tag{7}$$

$$\left(\frac{K_{hnf}}{K_f} + Rd\right)\theta'' + \frac{\left(\rho c_p\right)_{hnf}}{\left(\rho c_p\right)_f}\Pr f\theta' + \Pr Ec\left(\frac{\sigma_{hnf}}{\sigma_f}Mf'^2 + \frac{\mu_{hnf}}{\mu_f}f''^2\right) + \Pr Q\theta = 0 \tag{8}$$

With non-dimensional boundary conditions are given as follows,

$$\left.\begin{array}{l} f' = 0, f = 1, \theta = 1, \ at \ \eta = 0 \\ f' \to 0, \theta \to 0 \ as \ \eta \to \infty \end{array}\right\} \tag{9}$$

The physical variables play a vital role in revealing the explosive interaction between fluid structures at a rigid surface, where the viscous frictional force is quantified as the skin friction coefficient, also referred to as the surface force.

Here, the dimensionless forms of the local Nusselt number and skin friction are provided.

$$C_f \mathrm{Re}_x^{\frac{1}{2}} = \frac{f''(0)}{\left(1-\phi_1\right)^{2.5}\left(1-\phi_2\right)^{2.5}}, Nu\mathrm{Re}_x^{-\frac{1}{2}} = -\left(\frac{K_{hnf}}{K_f} + Rd\right)\theta'(0) \tag{10}$$

and $\mathrm{Re}_x\left(=\frac{(g\beta_T A)^{\frac{1}{2}}x}{\upsilon_f}\right)$ is referred as Reynolds number.

3 Mathematical formulation of entropy generation

In the system, entropy generation dissipates the available energy. Therefore, understanding the rate of entropy generation is crucial for enhancing the energy efficiency and overall system performance. Entropy generation for this problem [21] is formulated considering various factors: heat transfer, viscous dissipation, joule heating, and porosity. The first term in Eq. (10) represents irreversibility due to heat transfer, the second term represents viscous dissipation, the third term accounts for the magnetic field effect on local entropy formation, and the fourth term represents the effect of porosity.

$$S_G''' = \frac{1}{T_\infty^2}\left[\frac{K_{hnf}}{K_f} + \frac{16\sigma^* T_\infty^3}{3K^* K_f}\right]\left(\frac{\partial T}{\partial y}\right)^2 + \frac{\mu_{hnf}}{T_\infty}\left(\frac{\partial u}{\partial y}\right)^2 + \frac{\sigma_{hnf}}{T_\infty}B_0^2 u^2 + \frac{\mu_{hnf}}{T_\infty K_p}u^2 \tag{11}$$

The characteristics entropy generation rate is $E_{G_o} = \frac{T_w - T_0}{T_\infty}\frac{(g\beta_T A)^{\frac{1}{2}}}{\upsilon_f}K_{nf}$.

Using Eq. (6), the entropy generation in non-dimensional form is expressed as follows,

$$\begin{aligned} N_s &= \frac{S_G'''}{E_{G_o}} = N_{ST} + N_{SFF} \\ &= \left\{\left(\frac{K_{hnf}}{K_f} + Rd\right)\alpha_1 \theta\prime^2\right\} + \frac{\rho_f}{\rho_{hnf}}\left\{\frac{\mu_{hnf}}{\mu_f}Brf''^2 + \frac{\sigma_{hnf}}{\sigma_f}MBrf'^2 + \frac{\mu_{hnf}}{\mu_f}KpBrf'^2\right\} \end{aligned} \tag{12}$$

In the above equation, N_s denotes the total entropy of the system, N_{ST} denotes the entropy number due to the thermal effect including thermal radiation and N_{SFF} denotes entropy number due to the fluid friction, magnetic field and porous term.$\alpha_1\left(=\frac{T_w - T_\infty}{T_\infty}\right)$ denote the temperature difference in the form of non-dimensional, $Br\left(=\frac{\rho_{hnf}}{k_{nf}}\frac{(g\beta_T A)x^2}{(T_w - T_\infty)}\upsilon_f\right)$ and denote the Brinkman number used to correlate the heat produced by dissipation and the computed heat.

The Bejan number, defined as the ratio of irreversibility of heat transfer to the total irreversibility due to fluid friction and heat transfer, plays a vital role [24]. Its primary function is to evaluate the irreversibility of heat transfer and fluid flow processes, defined locally at every point of the boundary layer.

$$Be = \frac{N_{ST}}{N_{ST} + N_{SFF}} = \frac{\text{The entropy generation due to the thermal irreversibility}}{\text{The total entropy generation}} \tag{13}$$

4 Flow chart for numerical method

4.1 Method of solution

Solving the problem with non-linear ordinary differential equations (ODEs) exactly is challenging. Therefore, the system of governing equations with boundary conditions is solved numerically using BVP4C solver, known for its robustness and accuracy as confirmed by various heat transfer papers. Equation 4 provides the asymptotic boundary condition, with the value of the similarity variable η_{max} is set as 3. The non-linear coupled boundary value problem (BVP) of 3rd order in f and the 2nd order in θ is then reformulated into a system of first-order simultaneous equations with five unknowns, which we consider $y_1 = f, y_2 = f', y_3 = f'', y_4 = \theta, y_5 = \theta'$. The deduced system of first-order equations is as follows:

$$y_1' = y_2 \tag{14}$$

$$y_2' = y_3 \tag{15}$$

$$y_3' = \varepsilon \frac{\mu_f}{\mu_{hnf}} \left(\left(\frac{\sigma_{hnf}}{\sigma_f} M + \frac{\mu_{hnf}}{\mu_f} Kp \right) y_2 - \frac{1}{\varepsilon} \frac{\rho_{hnf}}{\rho_f} \left(y_1 y_3 - y_1^2 \right) \right) \tag{16}$$

$$y_4' = y_5 \tag{17}$$

$$y_5' = -\frac{1}{\left(\frac{k_{hnf}}{k_f} + Rd \right)} \left(\frac{\left(\rho c_p \right)_{hnf}}{\left(\rho c_p \right)_f} \Pr y_1 y_5 + \Pr Ec \left(\frac{\sigma_{hnf}}{\sigma_f} M y_2^2 - \frac{\mu_{hnf}}{\mu_f} y_3^2 \right) + \Pr Q y_5 \right) \tag{18}$$

and the corresponding boundary conditions are,

$$y_2(0) = 1,\ y_1(0) = \delta_1,\ y_4(0) = 1,\ y_2(\infty) = \delta_2,\ y_4(\infty) = \delta_3 \tag{19}$$

Utilizing the shooting method, initial values are guessed, then the resulting 5th order differential equations were solved by BVP4C with a step size of h = 0.01. The entire procedure is iteratively repeated until the desired result is obtained with a degree of accuracy of 10^{-5}. To ensure accuracy and reliability, the following convergence criteria are implemented: the absolute tolerance 'AbsTol' is set to 1e−5 to control the absolute error and ensure solution precision, while the relative tolerance is specified as 1e−4 to manage variations in the solution and achieve convergence. These convergence criteria collectively govern the termination condition for the iterative solution process. The chosen tolerance and iteration limits are determined based on the problem, aiming to achieve a satisfactory balance between solution accuracy and computational efficiency.

5 Results and discussions

In the analysis, the nanoparticle volume fraction (ϕ) varied between 1 and 4%, while the radiation parameter (Rd) ranging from 1 to 3 was observed to significantly affect the temperature distribution within the system. The Brinkman number (Br), magnetic parameter (M), heat source/sink parameter (Q), Eckert number (Ec), and porosity term (ε) were investigated within the ranges of 0–2, 1–3, 0.1–0.3, 0.1–0.3, and 1–3, respectively.

Table 1 The properties of hybrid nanoparticles and nanomaterials are taken from Fazle et al. [23] and Hussain et al. [30], and are listed in this table (with the shape of the nanoparticles considered here as 3.7)

Properties	Hybrid nanofluid
Density	$\rho_{hnf} = \rho_f(1-\varphi_2)\left\{(1-\varphi_1)+\frac{\varphi_1\rho_{s_1}}{\rho_f}\right\}+\varphi_2\rho_{s_2}$ *with* $\rho_{nf} = \rho_f(1-\varphi_2)(1-\varphi_1)+\varphi_1\rho_{s_1}$
Heat capacitance	$(\rho c_p)_{hnf} = (\rho c_p)_f(1-\varphi_2)\left\{(1-\varphi_1)+\frac{\varphi_1(\rho c_p)_{s_1}}{(\rho c_p)_f}\right\}+\varphi_2(\rho c_p)_{s_2}$ *with* $(\rho c_p)_{nf} = \rho_f(1-\varphi_2)(1-\varphi_1)+\varphi\rho_{s_1}$
Dynamic viscosity	$\mu_{hnf} = \mu_f\frac{1}{(1-\varphi_1)^{2.5}(1-\varphi_2)^{2.5}}$ *with*, $\mu_{nf} = \mu_f\frac{1}{(1-\varphi_1)^{2.5}}$,
Thermal conductivity	$k_{hnf} = k_{nf}\frac{k_{s_2}+(m-1)k_{bf}-(m-1)\varphi_2(k_{nf}-k_{s_2})}{(k_{s_2}+2k_{nf})+\varphi_2(k_{nf}-k_{s_2})}$, $k_{nf} = k_f\frac{k_{s_1}+(m-1)k_f-(m-1)\varphi_1(k_f-k_{s_1})}{k_{s_1}+(m-1)k_f-\varphi_1(k_f-k_{s_1})}$
Electrical conductivity	$\frac{\sigma_{hnf}}{\sigma_{nf}} = \frac{\sigma_{s_2}(1+2\varphi_2)+2\sigma_{nf}(1-\varphi_2)}{\sigma_{s_2}(1-\varphi_2)+\sigma_{bf}(2+\varphi_2)}$, $\frac{\sigma_{nf}}{\sigma_f} = \frac{\sigma_{s_1}(1+2\varphi_1)+2\sigma_f(1-\varphi_1)}{\sigma_{s_1}(1-\varphi_1)+\sigma_f(2+\varphi_1)}$

Table 2 Physical properties value is taken from the Fazle et al. [23] work

Fluid properties	$C_p\left(\frac{J}{Kg\,K}\right)$	$\rho\left(\frac{Kg}{m^3}\right)$	$k\left(\frac{W}{m\,K}\right)$	Pr	$\sigma\left(\frac{\Omega}{m}\right)$
Graphene oxide (GO)	717	1800	5000	–	6.30×10^7
Molybdenum disulphide (MoS_2)	397.746	5060	904.4	–	2.09×10^4
Water (base fluid)	4179	997.1	0.613	6.2	0.005

Table 3 The skin friction across different values of M when Rd = Q = Ec = 0

M	Xu and Lee [26]	Hayat et al. [25]	Mabood et al. [23]	Hussain et al. [30]	Present result
0	–	1.00000	1.00000	1.00000	1.00000
1	−1.41421	−1.41421	−1.41421	−1.41301	−1.415958
5	−2.4494	−2.44948	−2.44948	−2.44806	−2.449495
10	−3.3166	−3.31662	−3.31662	−3.31409	−3.316625
50	−7.1414	−7.14142	−7.14142	−7.14081	−7.141429
100	−10.0498	−10.04987	−10.04987	−10.0460	−10.049876
500	−22.38302	−22.38302	−22.38302	−22.3815	−22.383031
1000	–	−31.63858	−31.63858	−31.6365	−31.638586

Table 4 Variation against M on Skin friction and Nusselt number for Hybrid nanofluid and nanofluid with the values of $\phi_1 = 0.01$, $\phi_2 = 0.005$, m = 3.7, Pr = 6.2, Rd = Ec = 0.1 and Q = 0.01

Properties		Skin friction			Nusselt number		
		$GO+MoS_2$	GO	MoS_2	$GO+MoS_2$	GO	MoS_2
M	0	−0.9521	−0.9614	−0.9503	1.5810	1.5693	1.5781
	0.5	−1.1756	−1.8776	−1.1731	1.3896	1.3721	1.3777
	1.0	−1.3667	−1.3811	−1.3635	1.2067	1.2026	1.2055

Table 5 Variation against M on Entropy and Bejan number for Hybrid nanofluid and nanofluid with the values of $\phi_1 = 0.01$, $\phi_2 = 0.005$, m = 3.7, Pr = 6.2, Rd = Ec = 0.1 and Q = 0.01

Properties		Entropy			Bejan number		
		$GO+MoS_2$	GO	MoS_2	$GO+MoS_2$	GO	MoS_2
M	0	0.8177	0.8063	0.8172	0.2955	0.3036	0.2963
	0.5	1.2597	1.2419	1.2577	0.1461	0.1507	0.1467
	1.0	1.7216	1.6971	1.7282	0.0817	0.0847	0.0822

Table 6 Variation against various parameters on Nusselt number for Hybrid nanofluid and nanofluid with the values of $\phi_1 = 0.01$, $\phi_2 = 0.005$, m = 3.7, Pr = 6.2, Rd = Ec = 0.1 and Q = 0.01

Properties		Nusselt Number		
		GO + MoS_2	GO	MoS_2
Q	0	1.5562	1.5451	1.5534
	0.1	1.3647	1.3575	1.3622
	0.2	1.1526	1.1503	1.1516
Rd	0.1	1.6060	1.5965	1.6033
	0.2	1.6701	1.6622	1.6679
	0.3	1.7309	1.7243	1.7291
Ec	0	1.7704	1.7545	1.7669
	2	−2.8784	−2.7939	−2.8672
	4	−7.5273	−7.3425	−7.5014

Furthermore, the physical and thermophysical properties of nanoparticles are detailed in Tables 1 and 2, respectively. Table 3 provides a comparative analysis of skin friction values obtained from different magnetic parameter (M) values, compared to earlier research. Notably, Table 4 highlights a significant finding: the skin friction for the hybrid nanofluid is observed to be lower than that of the mono-fluid, while simultaneously, the heat transmission rate of the hybrid nanofluid exceeds that of the mono-fluid. This observation is crucial in understanding the enhanced heat transfer capabilities of the hybrid nanofluid system. Furthermore, Table 5 demonstrates that adjusting the emerging parameters can effectively reduce entropy generation, leading to a notable increase in the Bejan number for the hybrid nanofluid. Additionally, Table 6 presents data confirming the hybrid nanofluid's higher heat transfer rate compared to the mono-fluid. These results are graphically depicted, with the hybrid nanofluid represented by dashed lines, Graphene Oxide (GO) by dotted lines, and Molybdenum Disulphide (MoS_2) by solid lines. The parameters are set as follows: ε = 1.2, M = α1 = Ec = Kp = 0.1, Br = 0.5, and Q = 0.01, ensuring consistent and controlled conditions for analysis.

The study further reveals variations in entropy generation and Bejan number across different values of emerging characteristics, including the magnetic parameter (M), radiation parameter (Rd), heat source variable (Q), porosity variable (ε), Brinkman number (Br), as well as velocity and temperature profiles. In Fig. 2, it is evident that the temperature of the hybrid nanofluid exceeds that of the mono-fluid. This finding emphasizes the potential of hybrid nanofluids in enhancing heat transfer efficiency. Researchers can utilize this insight to optimize heat transfer processes.

Thermal radiation as one of the mode of heat transmission in the form of electromagnetic waves, influences the heat transfer within fluid particles, there by increasing it. From these physical aspects, higher values of Rd, as depicted in Fig. 3a and b, lead to increase temperature and Nusselt number profiles for the hybrid nanofluid compared to the mono-fluid. With an increase in the radiation parameter value, there is a corresponding rise in entropy. To reduce this increase in entropy, control over the Rd parameter becomes essential, as demonstrated in Fig. 3c. The enhancement of the radiation parameter strengthens the growth in the Bejan profile, as shown in Fig. 3d. The rise in the Bejan profile is caused by the dominance of fluid friction irreversibility resulting from heightened thermal radiation.

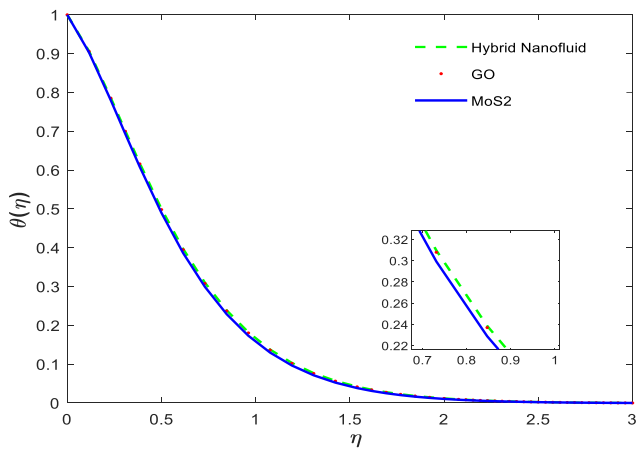

Fig. 2 Temperature profile for the nanofluid and hybrid nanofluid

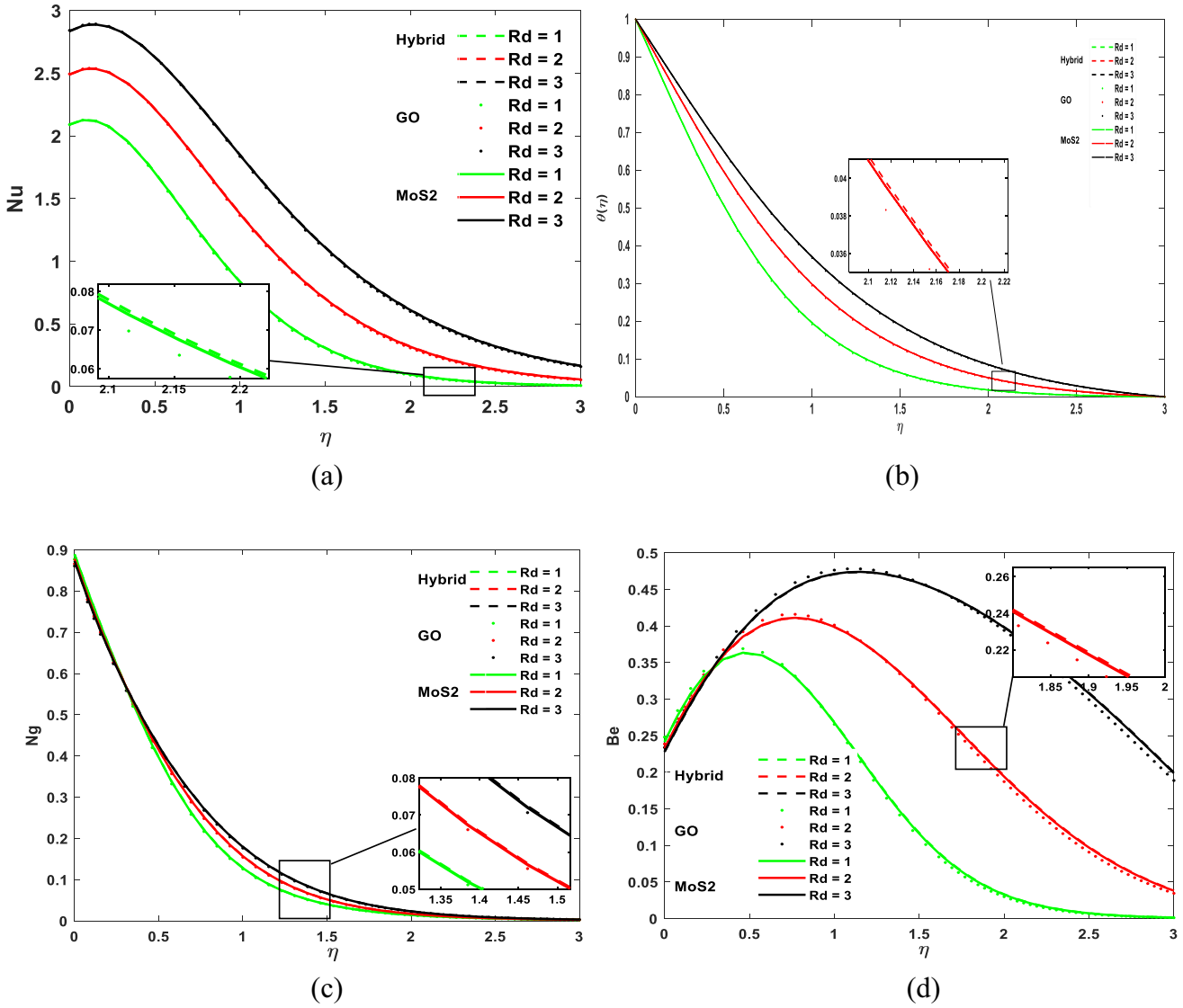

Fig. 3 **a**–**d** Impact of radiation parameter with Nusselt, Temperature, Entropy and Bejan profiles

The Brinkman number measures the significance of viscous heat relative to conductive heat transfer by comparing the heat generated through viscous dissipation where in fluid motion converts energy into internal energy to the heat transferred via molecular conduction. As illustrated in Fig. 4a, viscous dissipation plays a primary role during the heating process, resulting in increased entropy generation in hybrid nanofluids compared to nanofluids alone. Thus, managing Br is essential to minimize entropy growth. From Fig. 4b, the value of Br decreases with the increasing Bejan number for hybrid nanofluid than the nanofluid, because fluid friction (that is viscous dissipation) is dominated so that Bejan profile gets reduced.

The temperature differences, depicted by parameter α1 in Fig. 5a, grow along with the thermal energy. This increase corresponds to a simultaneous rise in entropy generation. Therefore, it is essential to regulate the temperature difference factors in order to decrease the entropy. The Bejan number in Fig. 5b represents the ratio between thermal irreversibility and total irreversibility. In the current context, an increase in the temperature difference parameter predominantly affects the numerator of the Bejan number. Consequently, for higher values of α1, the Bejan profile strengthens.

The porous medium is made up of pores or voids that contain the fluids. More holes in a medium will cause the fluid to flow slower because they restrict the flow of fluid as it passes through them. Meanwhile, thermal energy is induced by a decrease in velocity. More pores lead to better thermal efficiency from the perspective of physical properties. Figure 6a,

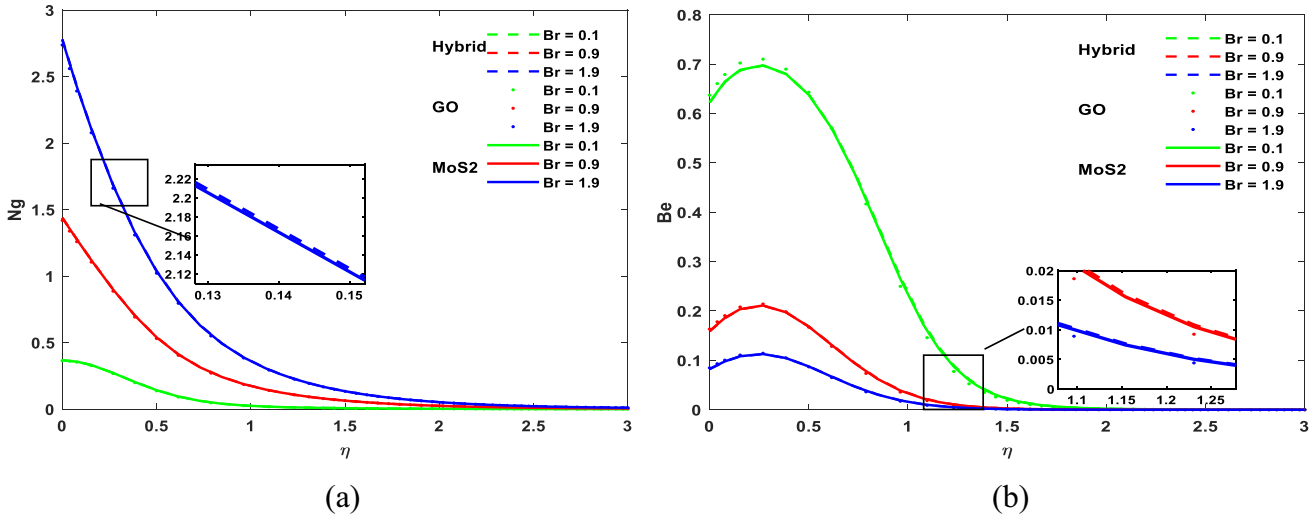

Fig. 4 **a**, **b** Impact of Br with entropy and Bejan profiles

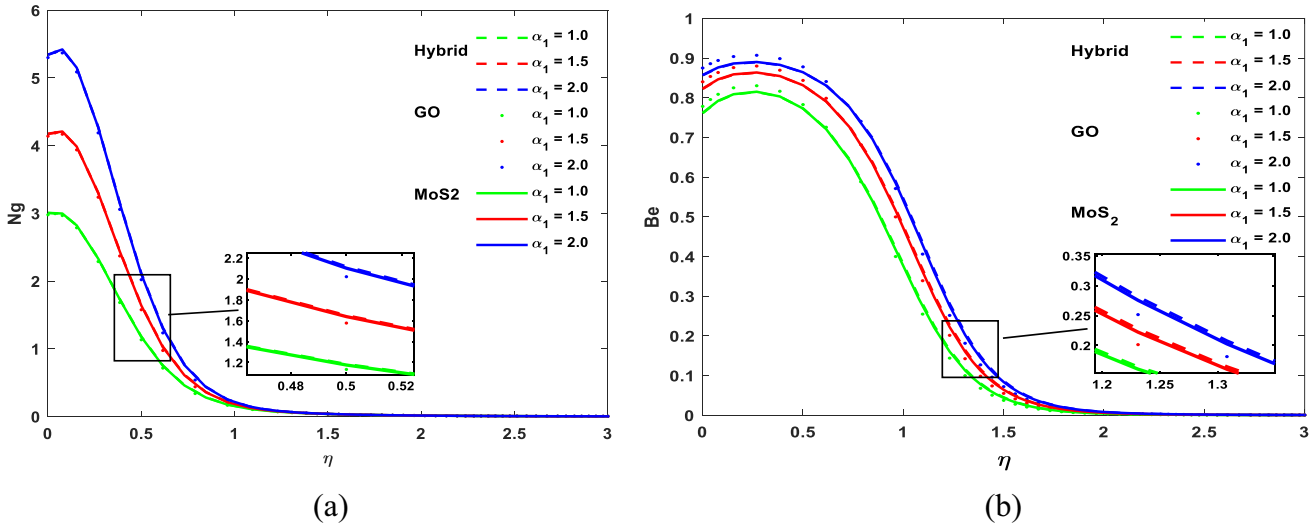

Fig. 5 **a**, **b** Impact of α_1 with entropy and Bejan profiles

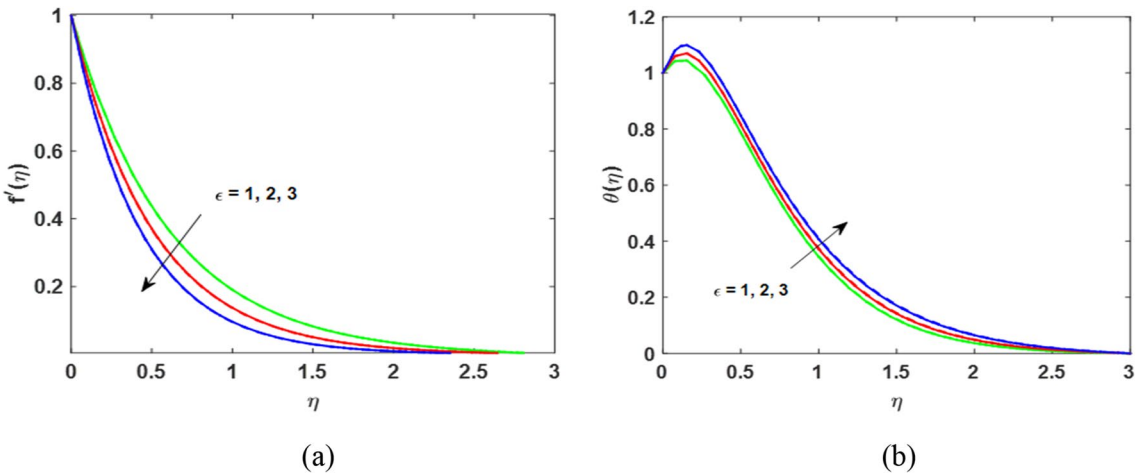

Fig. 6 **a**, **b** Impact of ε with velocity and temperature profiles

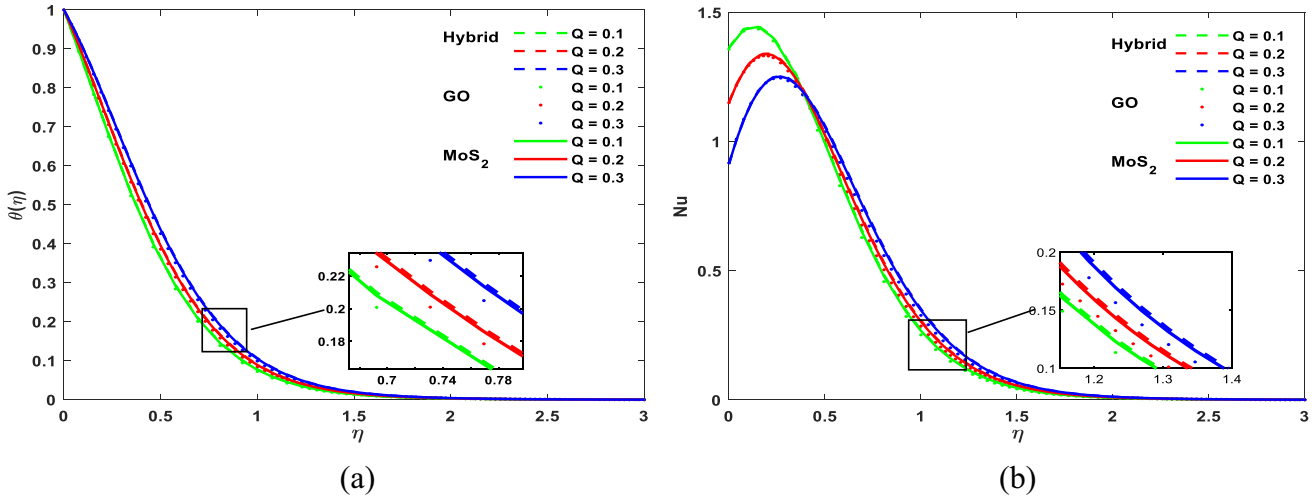

Fig. 7 **a**, **b** Impact of Q with Temperature and Nusselt profiles

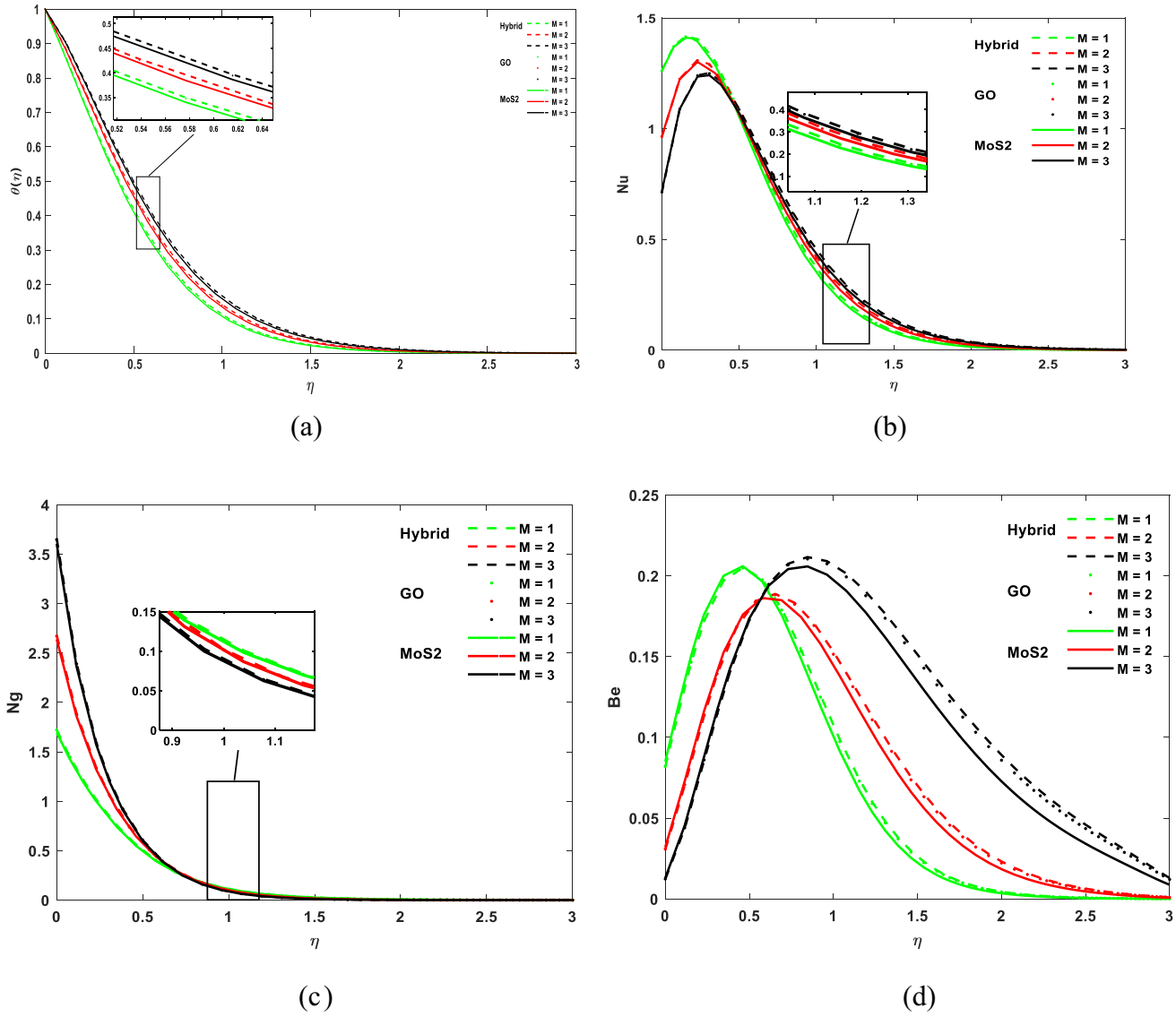

Fig. 8 **a**–**d** Impact of Magnetic parameter for the Temperature, Nusselt, Entropy and Bejan profiles

b provide a solid explanation of the above-mentioned concept, demonstrating that the hybrid nanofluid exhibits higher heat transfer rate compared to the mono-fluid.

The heat source parameter determines the heat transfer rate. Figure 7a, b demonstrate that, related to the mono-fluid, the temperature and Nusselt profile of the hybrid nanofluid are greater for larger values of Q (the heat source parameter) because an increase in Q also increases the heat transfer rate.

Magnetic parameter cause (resistive force) like a drag force because it acts against the direction of the motion of the fluid magnetic field refer exerts a force on a particle, is also named as Lorenz force. At that point, the fluid becomes subjected to increased magnetic influences, which cause frictional forces to remain constant. When friction increases, thermal energy also increases. Figure 8a, b illustrate that, in comparison to mono-fluids, the heat transfer rate for hybrid nanofluids increases as the magnetic parameter value increases. Entropy increases for the higher values of M, but entropy is minimized when it reaches the surface for the higher values of M. Because the magnetic field applied to the moving fluid flow produces a resistance for the moving fluid particle which creates some disorder in the flow. The mono-particle also has better control over entropy than the hybrid nanoparticle. However, the Bejan profile displays the inverse trend because a rise in magnetic force causes an increase in fluid friction, which in turn causes a reduction in pressure due

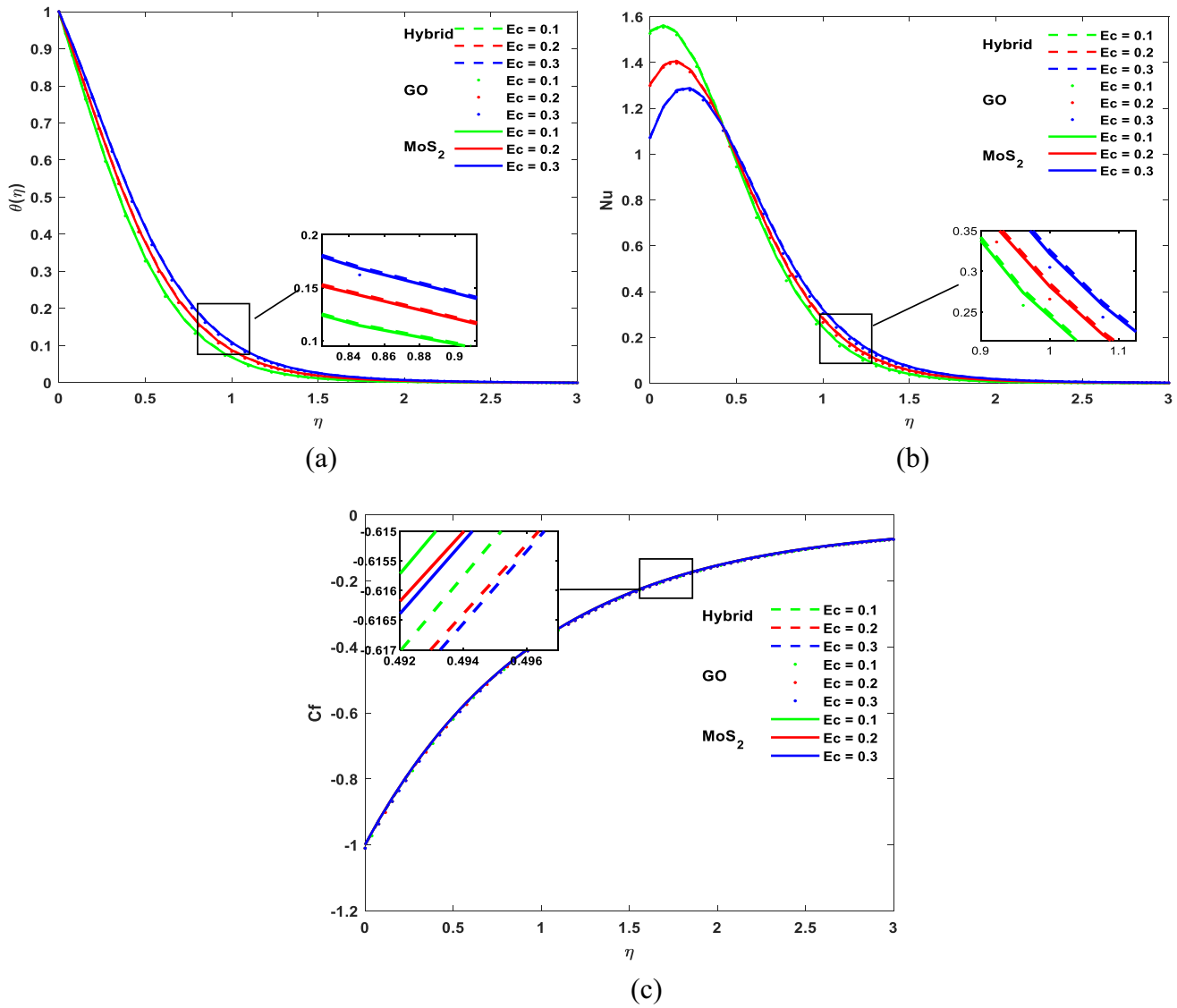

Fig. 9 **a**–**c** Impact of Eckert number with Temperature, Nusselt and Skin friction profiles

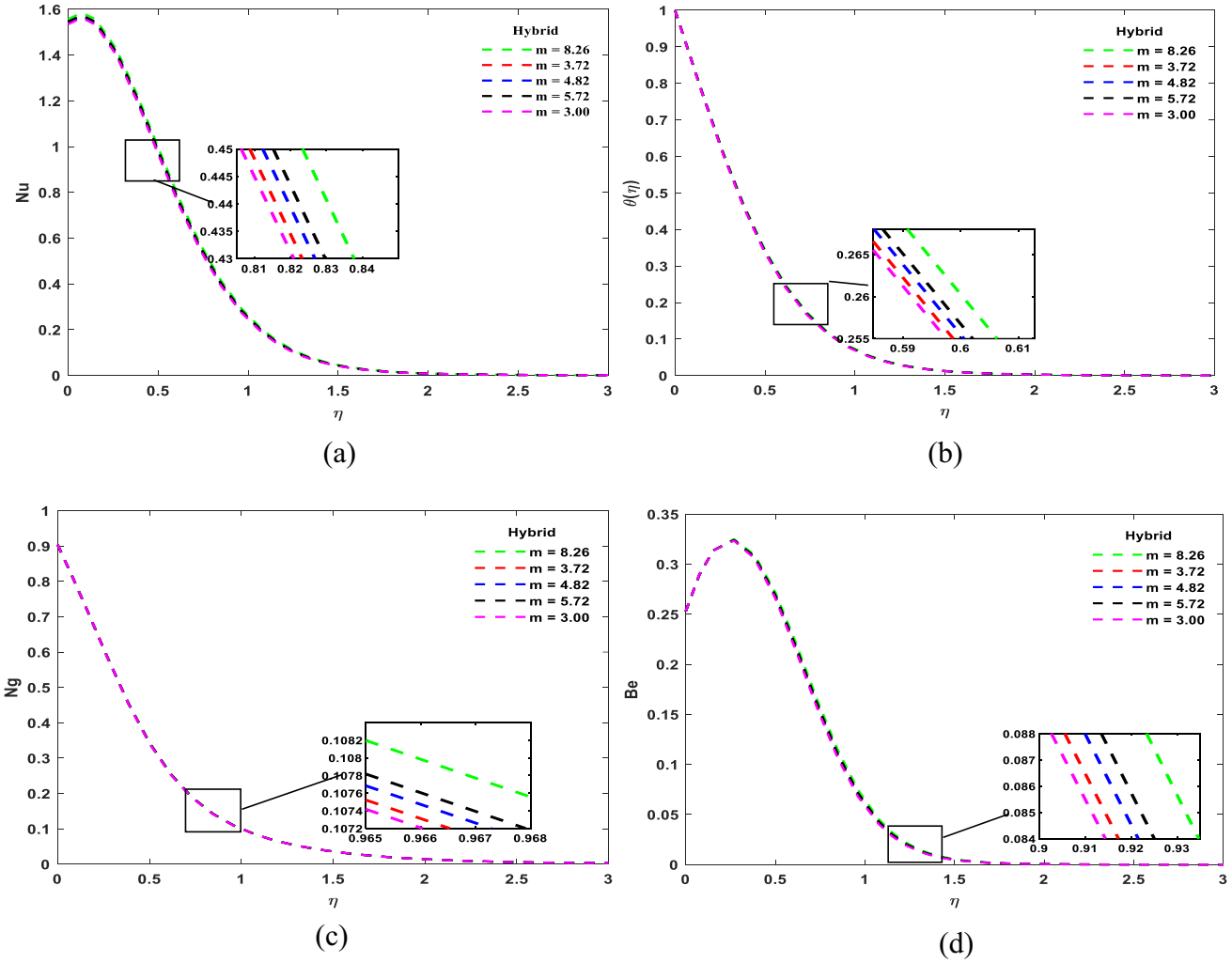

Fig. 10 a–d Impact of various shapes with Nusselt, Temperature,Entropy and Bejan profiles

to resistance in the flow of fluid. In order to maximize system performance and minimize energy usage, pressure drop minimizing is essential. Illustrations Fig. 8c, d make the above concepts crystal evident.

The Eckert number tells us how much the flow's kinetic energy fluctuates from the variation in enthalpy across the thermal boundary layer. Viscosity loss is a key component of understanding how heat spreads through high-speed flows. It's used to characterise the phenomenon of heat dissipation in high-speed flows, where in the impact of viscosity important. The rate of heat transmission can be enhanced by increasing Eckert number, which not only accelerates the velocity but also simulates the self-heating-up process. As clearly depicted in Figs. 9a, b, the heat transfer rate is higher for the hybrid nanofluid than the mono-fluid for the higher Eckert number. Because an increase in the Eckert number causes the fluid to flow faster, the skin friction with the fluid decreases as the number increases. When a fluid comes into contact with a solid surface, one traditional technique to measure the resistance to motion is skin friction. Compared to mono-fluid skin friction, hybrid nanofluid skin friction is reduced in this case. And may see that in Fig. 9c. Here, the various shapes of the nanoparticles were considered to determine which shape of the particle gave the best performance. And the values considered for m are 8.26, 3.2, 4.82, 5.72, 3.00 for blade, brick, cylinder, platelets and sphere respectively.

Figure 10a demonstrate the Nusselt profile with various shapes of the hybrid nanoparticles. It displays the flow of heat transmission rate. Also, it provides a measurement of the convective heat transfer that takes place at the surface level. In physical terms, the Nusselt number is the ratio of convective heat transmission to conductive heat transfer. So, the blade-shaped nanoparticle has a higher rate of heat transmission than the others is described in Fig. 10b. Figure 10c depicts the entropy production for the various shapes of the nanoparticles. Minimizing

entropy generation increases thermal efficiency. This picture clearly says that the sphere shape of the nanoparticle reduces entropy generation compared to the other shapes of the nanoparticle. From a physical perspective, a low Bejan number enhances the heat transfer rate since it determines a proportion of heat transmission irreversibility compared to the total proportion of heat transfer and fluid friction-induced irreversibility. Figure 10d shows that the sphere-shaped nanoparticle has greater thermal efficiency than the other shape of the nanoparticle.

6 Conclusion

This study investigates entropy generation in hybrid nanofluid flow incorporating magnetohydrodynamic, thermal radiation, and ohmic viscous dissipation phenomena over a stretching sheet. Graphene Oxide (GO) and Molybdenum Disulphide (MoS_2) are employed as hybrid nanoparticles dispersed in water, serving as the base liquid. Entropy generation analysis helps in determining the irreversibility and inefficiencies present in a system. The system of governing equations is solved using MATLAB bvp4c solver. The behavior of the various emerging parameters has been explained and analyzed graphically. The primary finding obtained from this study are summarized as follows:

a. The heat transmission rate is observed to be higher for the hybrid nanofluid compared to the mono-fluid.
b. Effective control of the temperature difference parameter, Rd (Radiation parameter), and Br (Brinkman number) is essential for minimizing the entropy generation rate.
c. Blade-shaped nanoparticles demonstrate superior heat transfer rates, whereas sphere-shaped nanoparticles contribute to reducing entropy production.

The results obtained from this study are significant for various biomedical fields and coolant mechanism research.

Acknowledgements The Authors Express their Appreciation to King Saud University for funding the publication of this research through the Researchers Supporting Project number (RSPD2024R1004), King Saud University, Riyadh, Saudi Arabia.

Author contributions Revathi devi M: Original Draft, Methodology, Formulation and Visualization, Funding Supporting, Narsu Sivakumar: Supervision Software, Formulation and Visualization, Nainaru Tarakaramu: editing and analyzing, formulation, Hijaz Ahmad and Sameh Askar: Formulation and Visualization, Funding Supporting.

Funding This project is funded by King Saud University, Riyadh, Saudi Arabia.

Data availability The data will be made available on a reasonable request to the corresponding author.

Declarations

Competing interests The authors declare no competing interests.

References

1. Choi SU, Eastman JA. Enhancing thermal conductivity of fluids with nanoparticles (No. ANL/MSD/CP-84938; CONF-951135–29). Argonne National Lab. (ANL), Argonne, IL (United States); 1995.
2. Wong KV, De Leon O. Applications of nanofluids: current and future. Adv Mech Eng. 2010. https://doi.org/10.1155/2010/519659.
3. Yu W, Xie H. A review on nanofluids: preparation, stability mechanisms, and applications. J Nanomater. 2012. https://doi.org/10.1155/2012/435873.
4. Shoaib M, Raja MAZ, Sabir MT, Awais M, Islam S, Shah Z, Kumam P. Numerical analysis of 3-D MHD hybrid nanofluid over a rotational disk in presence of thermal radiation with Joule heating and viscous dissipation effects using Lobatto IIIA technique. Alex Eng J. 2021;60(4):3605–19. https://doi.org/10.1016/j.aej.2021.02.015.
5. Ratha PK, Mishra S, Tripathy R, Pattnaik PK. Analytical approach on the free convection of Buongiorno model nanofluid over a shrinking surface. Proc Inst Mech Eng Part N J Nanomater Nanoeng Nanosyst. 2022;237(3–4):83–95. https://doi.org/10.1177/23977914221103982.

6. Mustafa T. Single phase nanofluids in fluid mechanics and their hydrodynamic linear stability analysis. Comput Methods Programs Biomed. 2020;187:105171. https://doi.org/10.1016/j.cmpb.2019.105171.
7. Masthanaiah Y, Tarakaramu N, Khan IM, Rushi Kesava A, Moussa SB, Fadhl BM, Abdullaev SS, Eldin SM. Impact of viscous dissipation and entropy generation on cold liquid via channel with porous medium by analytical analysis. Case Stud Therm Eng. 2023;47:103059. https://doi.org/10.1016/j.csite.2023.103059.
8. Mahesh R, Mahabaleshwar US, Kumar VPN, Öztop HF, Abu-Hamdeh N. Impact of radiation on the MHD couple stress hybrid nanofluid flow over a porous sheet with viscous dissipation. Results Eng. 2023;17:100905. https://doi.org/10.1016/j.rineng.2023.100905.
9. Sharma K, Kumar S, Vijay N. Insight into the motion of Water-Copper nanoparticles over a rotating disk moving upward/downward with viscous dissipation. Int J Mod Phys B. 2022. https://doi.org/10.1142/S0217979222502101.
10. Rashad AM, Nafe MA, Eisa DA. Heat variation on MHD Williamson hybrid nanofluid flow with convective boundary condition and ohmic heating in a porous material. Sci Rep. 2023;13:6071. https://doi.org/10.1038/s41598-023-33043-z.
11. Yaseen M, Rawat SK, Kumar M. Hybrid nano fluid (MoS_2–SiO_2/water) flow with viscous dissipation and ohmic heating on an irregular variably thick convex/concave-shaped sheet in a porous medium. Heat Transf. 2022;51(1):789–817. https://doi.org/10.1002/htj.22330.
12. Puneeth V, Manjunatha S, Makinde OD, Gireesha BJ. Bioconvection of a radiating hybrid nanofluid past a thin needle in the presence of heterogeneous–homogeneous chemical reaction. ASME J Heat Transf. 2021;143(4):042502. https://doi.org/10.1115/1.4049844.
13. Nayak B, Acharya S, Mishra SR. Impact of dissipative heat and thermal radiation on the steady magnetohydrodynamic nanofluid flow with an interaction of Brownian motion and chemical reaction. Int J Appl Comput Math. 2022;8(3):1–18. https://doi.org/10.1007/s40819-022-01345-x.
14. Mustafa M, Khan JA, Hayat T, Alsaedi A. Buoyancy effects on the MHD nanofluid flow past a vertical surface with chemical reaction and activation energy. Int J Heat Mass Transf. 2017;108:1340–6. https://doi.org/10.1016/j.ijheatmasstransfer.2017.01.029.
15. Krishna MV, Ahammad NA, Chamkha AJ. Radiative MHD flow of Casson hybrid nanofluid over an infinite exponentially accelerated vertical porous surface. Case Stud Therm Eng. 2021;27:101229. https://doi.org/10.1016/j.csite.2021.101229.
16. Nandi S, Das M, Kumbhakar B. Entropy generation in magneto-Casson nanofluid flow along an inclined stretching sheet under porous medium with activation energy and variable heat source/sink. J Nanofluids. 2022;11(1):17–30. https://doi.org/10.1166/jon.2022.1823.
17. Qureshi MZA, Bilal S, Ameen MB, Mushtaq T, Malik MY. Numerical examination about entropy generation in magnetically effected hybridized nanofluid flow between orthogonal coaxial porous disks with radiation aspects. Surf Interfaces. 2021;26:101340. https://doi.org/10.1016/j.surfin.2021.101340.
18. Abad JMN, Alizadeh R, Fattahi A, Doranehgard MH, Alhajri E, Karimi N. Analysis of transport processes in a reacting flow of hybrid nanofluid around a bluff-body embedded in porous media using artificial neural network and particle swarm optimization. J Mol Liq. 2020;313:113492. https://doi.org/10.1016/j.molliq.2020.113492.
19. Bejan A. The thermodynamic design of heat and mass transfer processes and devices. Int J Heat Fluid Flow. 1987;8(4):258–76. https://doi.org/10.1016/0142-727X(87)90062-2.
20. Bejan A. A study of entropy generation in fundamental convective heat transfer. J Heat Transf. 1979;101(4):718–25. https://doi.org/10.1115/1.3451063.
21. Baag S, Mishra SR, Dash GC, Acharya MR. Entropy generation analysis for viscoelastic MHD flow over a stretching sheet embedded in a porous medium. Ain Shams Eng J. 2017;8(4):623–32. https://doi.org/10.1016/j.asej.2015.10.017.
22. Pal D, Das BC, Vajravelu K. Magneto-Soret-Dufour thermo-radiative double-diffusive convection heat and mass transfer of a micropolar fluid in a porous medium with ohmic dissipation and variable thermal conductivity. Propuls Power Res. 2022;11(1):154–70. https://doi.org/10.1016/j.jppr.2022.02.001.
23. Mabood F, Mastroberardino A. Melting heat transfer on MHD convective flow of a nanofluid over a stretching sheet with viscous dissipation and second order slip. J Taiwan Inst Chem Eng. 2015;57:62–8. https://doi.org/10.1016/j.jtice.2015.05.020.
24. Bejan A. Entropy generation through heat and fluid flow. New York: Wiley; 1982.
25. Hayat T, Hussain Q, Javed T. The modified decomposition method and Pade approximation for the MHD flow over a non-linear stretching sheet. Nonlinear Anal Real World App. 2009;10:966–73. https://doi.org/10.1016/j.nonrwa.2007.11.020.
26. Xu L, Lee EWM. Variational iteration method for the magnetohydrodynamic flow over a nonlinear stretching sheet. Abstr Appl Anal. 2013. https://doi.org/10.1155/2013/573782.
27. Khan MI, Alzahrani F. Free convection and radiation effects in nanofluid (silicon dioxide and Molybdenum disulfide) with second order velocity slip, entropy generation, Darcy-Forchheimer porous medium. Int J Hydrog Energy. 2020;46(1):1362–9. https://doi.org/10.1016/j.ijhydene.2020.09.240.
28. Ghadikolaei S, Gholinia M. 3D mixed convection MHD flow of GO-MoS_2 hybrid nanoparticles in H_2O–$(CH_2OH)_2$ hybrid base fluid under the effect of H_2 bond. Int Commun Heat Mass Transf. 2019;110:104371. https://doi.org/10.1016/j.icheatmasstransfer.2019.104371.
29. Arif M, Kumam P, Khan D, Watthayu W. Thermal performance of GO-MoS_2/engine oil as Maxwell hybrid nanofluid flow with heat transfer in oscillating vertical cylinder. Case Stud Therm Eng. 2021;27:101290. https://doi.org/10.1016/j.csite.2021.101290.
30. Hussain Z, Alshomrani AS, Muhammed T, Anwar MS. Entropy analysis in mixed convective flow of hybrid nanofluid subject in mixed convective flow of hybrid nanofluid subject to melting heat and chemical reactions. Case Stud Therm Eng. 2022;34:101972. https://doi.org/10.1016/j.csite.2022.101972.